

## EDDY CURRENT IMAGE RESTORATION USING THE GROSHONG PARAMETRIC MODEL

T. Sollier, J.-M. Philippe, H. Maury  
Commissariat à l'Energie Atomique (CEA)  
Centre d'Etudes et de REcherches sur les Matériaux (CEREM)  
Service des Techniques Avancées (STA)  
CEA Saclay, 91191 Gif-sur-Yvette Cedex, FRANCE

D. Villard  
Electricité de France (EdF)  
Direction des Etudes et Recherches (DER)  
Département Etude des Matériaux (DEM)  
Les Renardières, 77250 Moret-sur-Loing, FRANCE

### INTRODUCTION

French PWR cooling systems include austenitic/ferritic stainless steel cast elbows. Due to the aging of these components, there is an increasing need for monitoring possible fabrication flaws near the elbow inner and outer surfaces. Various non destructive techniques are being evaluated by the EdF (French Electricity Board) for defect detection and characterization. One of these, the eddy current (EC) technique, is usually very efficient for the detection of flaws near the surface. However, large local variations in the ferrite ratio induce high structural noise thus reducing the EC detection efficiency. Image restoration using the Groshong parametric model is proposed as a means of improving the signal-to-noise ratio (SNR) and defect characterization.

### GROSHONG EC TRANSDUCER MODEL

The Groshong EC transducer model [1, 2] is simply based on a weighted sum of the path lengths of an annulus of eddy current filaments flowing on the component surface and is suitable for axially symmetric probes. In a general form, the transducer response can be written as:

$$G = H_p \{F\} + N, \quad (1)$$

where  $G$  is the image obtained from the probe impedance changes when scanned over the component surface,  $H_p$  the nonlinear transfer function of the probe defined by the parameters  $p$ ,  $F$  the original flawed surface image and  $N$  the noise. The noise is assumed to be additive in Groshong's publications and in the work presented here. This assumption seems reasonable on the basis of experimental data for aluminum and cast stainless steel blocks.

For a polar coordinate system centered on the probe axis, the transfer function  $H_p$  is expressed by a layered nonlinear representation including 2 convolutions and a nonlinear point function:

$$H_p\{F\} = \sum_{k=0}^{K-1} h_{(k)}^1 * s^1(h_{(k)}^0 * F), \tag{2}$$

where the layer  $h_{(k)}^0$  approximates locally the current filament deviation caused by a flaw. The function  $s^1$  is used to express the current filament path length locally and is a nonlinear point function depending on the nonlinear experimental transducer response. The layer  $h_{(k)}^1$  is used to integrate the path length weighted by the current density over the radius of the transducer. The summation over  $k$  is the discrete formulation for the angular integration of the current path lengths. Detailed formulations of these functions are given in Groshong's Ph.D. thesis [3]. The function  $s^1$  defined by Groshong has been modified to remove the DC component :

$$s^1(x) = \sqrt{1+x^2} - 1. \tag{3}$$

### DETERMINATION OF THE MODEL PARAMETERS

Groshong's model is an empirical model of an axially symmetric EC probe and thus the parameters, denoted  $p$ , have to be adjusted using experimental data. Groshong estimates the point spread function (PSF) of the transducer from a sampled image of a small diameter hole in a non-ferrous block. But the evaluation of some parameters is not detailed and cannot be directly linked to the probe geometry and to the PSF. A standard signal processing tool has been used to set the parameters of our probe: a minimum mean square error algorithm (MMSE) [4] with constraints on the parameters  $p$ . The estimate of these for the minimum mean square error criterion is expressed as:

$$\hat{p} = \arg \min_p \left( \|G - H_p\{F\}\|^2 \right). \tag{4}$$

In practice, the cost function in equation (4) has many local minima. Therefore, deterministic optimization processes such as the gradient descent or simplex would not provide the global minimum. A stochastic optimization method is thus required to escape from local minima: simulated annealing [5] has been used. This procedure converges towards a low cost solution which seems satisfactory to achieve our inversion goal even if it is not the actual solution. The model identification result for a cross-shaped electrical discharge machined (EDM) notch on an aluminum block is shown in Figure 2.

The estimation algorithm can be described as follows:

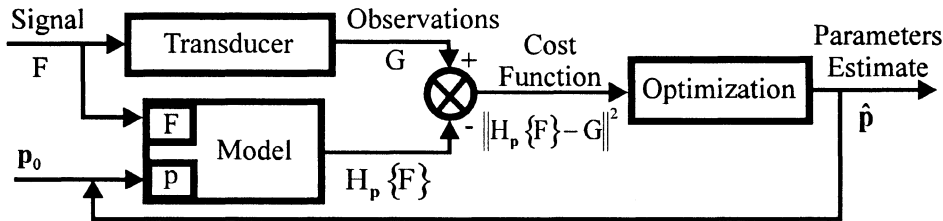


Figure 1. Algorithm for estimation of Groshong model parameters.

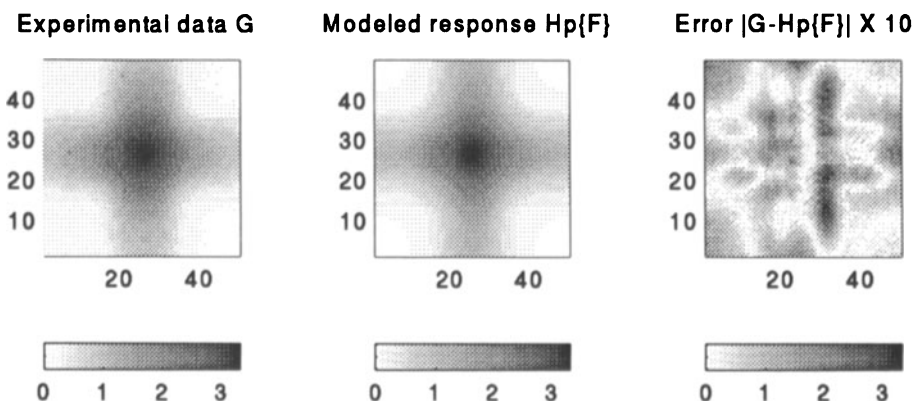


Figure 2. Estimation of Groshong model parameters for an EDM notch in aluminum, from left to right : experimental data, modeled response and absolute error multiplied by 10.

## IMAGE RESTORATION WITH GAUSSIAN WHITE NOISE

### Maximum Likelihood

As a first step in the development and evaluation of the inverse methods efficiency for image restoration, we consider Gaussian white noise. Noisy signals with a different power spectral density (PSD) are discussed below. Image restoration is first performed with the *maximum likelihood* method (ML) as used by Groshong. The *maximum likelihood* method gives the original flawed surface  $F$  that maximizes the probability distribution of the observations (experimental data  $G$ ). In other words,  $G$  is the most likely image for a given  $F$ . Using this criterion, the estimate of  $F$ , denoted  $\hat{F}_{ML}$  is :

$$\hat{F}_{ML} = \arg \max_F \{p(G|F)\}, \quad (5)$$

where  $p(G|F)$  is the probability distribution of  $G$  for a given  $F$ . For an additive Gaussian white noise, the equation (5) is equivalent to minimizing the quadratic error [6]:

$$\hat{F}_{ML} = \arg \min_F \left\{ \|G - H_p \{F\}\|^2 \right\}. \quad (6)$$

The Groshong model accepts an analytical formulation for its gradient that significantly speeds up the optimization algorithm. Thus, like Groshong, we used an iterative gradient descent to minimize the cost function. To ensure convergence of the restoration algorithm, Groshong incorporates *a priori* information on the solution  $\hat{F}_{ML}$  by adding constraints. The constraints are: i), the image pixels have positive values, ii), the Euclidean norm of the estimate tends to zero (without flaws,  $F$  should be the null matrix) and iii), a "spectral magnitude clipping" is gradually relaxed in the restoration process. The "spectral magnitude clipping" is a low pass filter used to help convergence of the inversion algorithm to a satisfactory solution. It turns out that its relaxation procedure is difficult to adjust and is dependent on the image shape. It requires the introduction of tuning *hyperparameters* [7] experimentally determined by tests performed on a set of flaws. We suggest in this work that the *a priori* information can be introduced more conveniently with a smaller number of *hyperparameters* by using the *maximum a posteriori* method (MAP).

## Maximum a posteriori

The *maximum a posteriori* method maximizes the probability distribution of the original signal (flawed surface F) given the observations (experimental data G). Thus, the estimate of F denoted  $\hat{F}_{\text{MAP}}$  is the most likely image for a given G. This Bayesian approach implies that we consider the solution as a random variable with some *a priori* information expressed by a probability distribution [8]. With respect to this criterion,  $\hat{F}_{\text{MAP}}$  is written as:

$$\hat{F}_{\text{MAP}} = \arg \max_F \{p(F|G)\}, \quad (7)$$

where  $p(F|G)$  is the probability distribution of F for a given G. Using Bayes' theorem and the logarithm function monotonicity we have :

$$\hat{F}_{\text{MAP}} = \arg \max_F \left\{ \log(p(G|F)) + \log(p(F)) \right\}. \quad (8)$$

For an additive Gaussian white noise and a Gaussian distribution for the image F, equation (9) is equivalent to [6]:

$$\hat{F}_{\text{MAP}} = \arg \min_F \left\{ \|G - H_p\{F\}\|^2 + \tau \mathbf{f}^T C_f^{-1} \mathbf{f} \right\}, \quad (9)$$

where  $\mathbf{f}$  is the column vector obtained by reshaping the matrix F,  $C_f$  is the covariance matrix of  $\mathbf{f}$  and  $\tau$  a weighting factor. The covariance matrix of  $\mathbf{f}$  is determined by the probability distribution over F. If the image F pixels were completely independent, the covariance matrix would be the identity matrix and the last term of equation (9) would simply be the Euclidean norm. In this case, the estimate would be force towards the null matrix, which is analogous to adding the norm constraint to the ML method. Note that the second term of equation (9) is often referred to as a *regularization* factor giving convex properties to the cost function, thus ensuring optimization technique efficiency and that the solution is unique.

## Modeling A Priori Knowledge of F

The *a priori* knowledge of the solution (i.e., the probability distribution over F) is modeled with a *Gauss-Markov random field* (GMRF) [9, 10]. We consider a first order GMRF involving only the four closest neighbors of a pixel  $f_{i,j}$ , without any preferential direction. This is reasonable since our transducer has an isotropic response and the pixels are not assumed to be time related (in fact, they are time related since the image comes from a line oriented scan of the material but we consider only spatial correlation between the image pixels). With respect to the sampling grid, the resolution of the transducer and the usual flaw geometry, a first order model seems also suitable to describe  $p(F)$ . This GMRF model can be represented as :

$$f_{i,j} + \sum_{|k|+|l|=1} a f_{i-k,j-l} = u_{i,j}, \quad (10)$$

where  $a$  is a parameter and  $\mathbf{u}$  is a Gaussian noise such as :

$$\begin{cases} E\{f_{i,j}u_{p,q}\} = \sigma^2 \delta_{ip} \delta_{jq} \\ E\{u_{i,j}u_{p,q}\} = \begin{cases} \sigma^2 & \text{if } (i,j) = (p,q), \\ -a\sigma^2 & \text{if } (|i-p| + |j-k| = 1), \\ 0 & \text{otherwise,} \end{cases} \end{cases} \quad (11)$$

It can be shown [11] that the parameter  $a$  should range from -0.25 to 0 to give a low pass PSD to  $F$ . The logarithm of the probability distribution over  $F$  can be written as a C-norm over  $f$  (equation (12)) and as a *Gibbs distribution* (equation (13)) :

$$\begin{aligned} \log(p(F)) + \text{constant} &= -\mathbf{f}^T \mathbf{C}_r^{-1} \mathbf{f}, \\ &= -\mathbf{f}^T \cdot (\mathbf{f} + \mathbf{C} * \mathbf{f}), \\ &= -\|\mathbf{f}\|_C^2, \end{aligned} \quad (12)$$

$$\text{where } \mathbf{C} = \begin{pmatrix} 0 & a & 0 \\ a & 0 & a \\ 0 & a & 0 \end{pmatrix},$$

$$\log(p(F)) = -\lambda \sum_{i,j} \left( f_{i,j}^2 + b \sum_{|k|+|l|=1} (f_{i,j} - f_{i-k,j-l})^2 \right), \quad (13)$$

$$\text{where } b = -\frac{a}{2(1+4a)} \geq 0 \text{ and } \lambda \text{ is a positive constant.}$$

$\mathbf{C}_r^{-1}$  is a symmetric positive definite matrix which thus defines a C-vector norm over  $f$ . Equation (12) shows that this norm can be written using a convolution product which highly simplifies computation of the cost function and its gradient, both of which are involved in the optimization process.

### Edge Restoration Enhancement

The quadratic cost of the GMRF tends to favor smooth transitions instead of restoring sharp edges that actual flaws have. Bouman[12] proposes a generalized Gaussian Markov random field (GGMRF) to overcome this limitation and introduces a generalized CQ-norm over  $f$ :

$$\|\mathbf{f}\|_{CQ}^Q = -\lambda \sum_{i,j} \left( |f_{i,j}|^Q + b \sum_{|k|+|l|=1} |f_{i,j} - f_{i-k,j-l}|^Q \right), \quad (14)$$

where  $Q$  is a scalar ranging from 1 to 2. We found  $Q=1.3$  convenient for our application.

### Synthetic Experiments

We tested the ML and MAP methods on synthetic data (figure 3). We added synthetic white Gaussian noise to the model response of a synthetic flaw in order to obtain a SNR of 7 dB. Despite the high noise level, we are able to restore roughly the shape of the flaw. *Hyperparameter* estimation was found to be much easier using the MAP method. Better contrast and sharper edges were also observed for the MAP estimate  $\hat{F}_{\text{MAP}}$ .

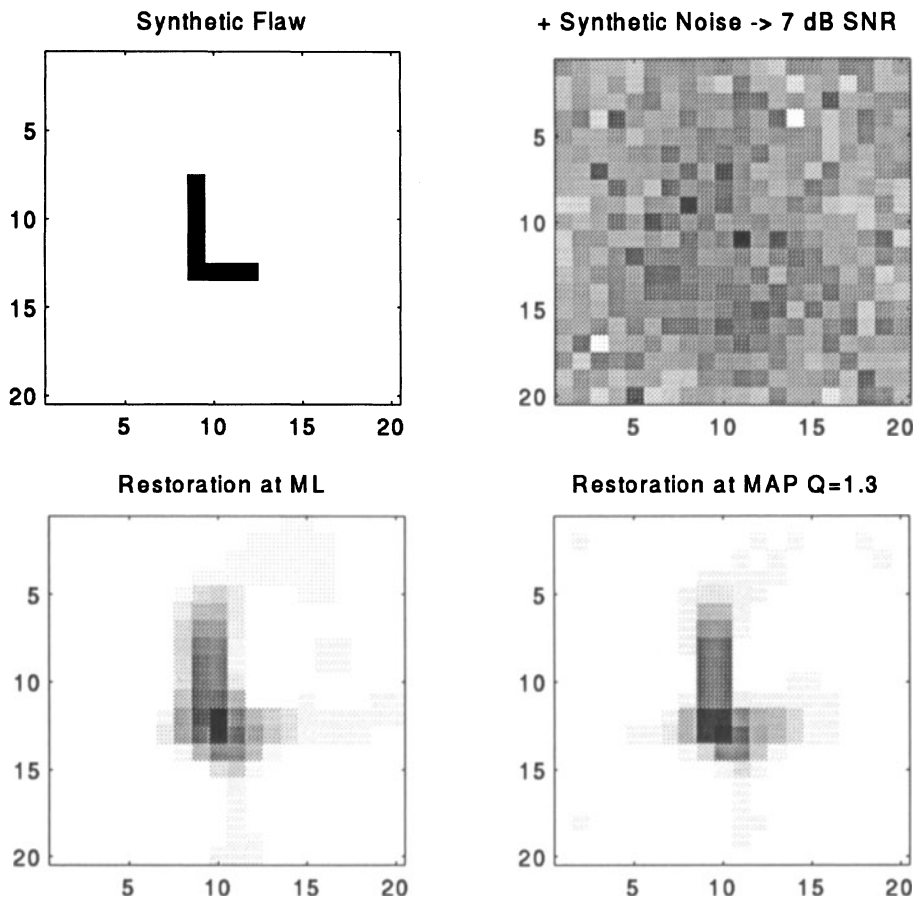


Figure 3. Image restoration of synthetic data, upper left: original data  $F$ , upper right : synthetic data  $G$  with additive white Gaussian noise, lower left: Maximum Likelihood restoration, lower right : Maximum *a posteriori* restoration.

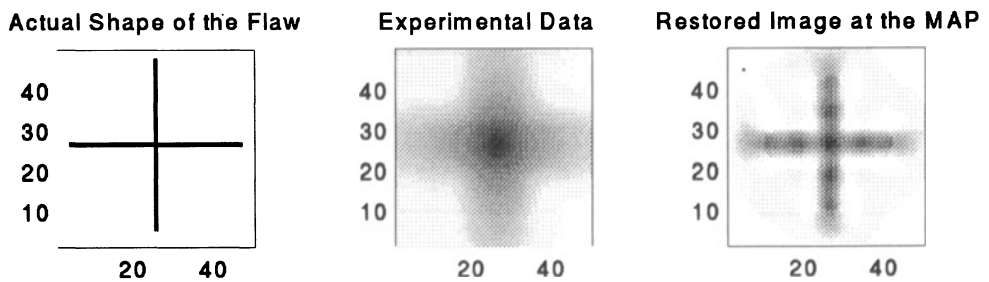


Figure 4. MAP image restoration for an EDM notch in an aluminum block, from left to right: original data  $F$ , experimental data  $G$  and MAP restored image.

## Experimental Results

We performed image restoration for a cross-shaped EDM notch in an aluminum block. The noise level is very low and can be regarded as Gaussian. The ML or MAP restored images are very similar and reliably reproduce the original flaw geometry (figure 4).

### IMAGE RESTORATION FOR CAST STAINLESS STEEL

For EC data for cast stainless steel, the noise can no longer considered to be white. We modeled it as a second order GMRF which can be easily implanted and can represent a wide class of signals. The GMRF coefficients are computed with two steps : i) the noise is first modeled as white Gaussian passing through a second order autoregressive (AR) filter with conjugate poles and the AR filter coefficients are experimentally adjusted in order to match the PSD of the actual noise, ii) the coefficients of a GMRF with a similar PSD are then computed from the AR filter characteristics. The estimate of  $F$  in this case becomes :

$$\hat{F}_{\text{MAP}} = \arg \min_F \left\{ \left( \mathbf{g} - \mathbf{H}_p \{ \mathbf{f} \} \right)^T \mathbf{V}_n^{-1} \left( \mathbf{g} - \mathbf{H}_p \{ \mathbf{f} \} \right) + \tau \mathbf{f}^T \mathbf{C}_r^{-1} \mathbf{f} \right\}, \quad (15)$$

$$\hat{F}_{\text{MAP}} = \arg \min_F \left\{ \left\| \mathbf{G} - \mathbf{H}_p \{ \mathbf{F} \} \right\|_{V_Q}^Q + \tau \left\| \mathbf{F} \right\|_{C_Q}^Q \right\}, \quad (16)$$

where  $\mathbf{V}_n$  is the covariance matrix of the noise  $\mathbf{N}$  reshaped in a column vector  $\mathbf{n}$  and modeled by a GMRF. Equation (15) represents a vector formulation and equation (16) a matrix formulation with  $V_Q$  and  $C_Q$  norm over  $F$ . The power  $Q$  corresponds to the GGMRF model as defined in equation (14).

## Experimental Results

We performed image restoration for EDM notches in a cast stainless steel block. The SNR was enhanced by preprocessing (basically optimal frequency mixing [13]). The MAP restored image reproduces the original flaw geometry.

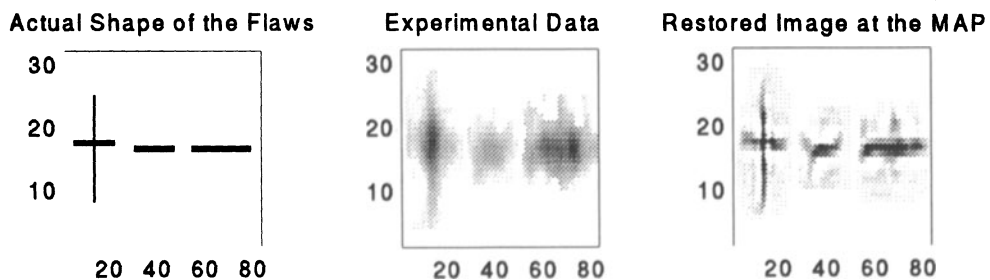


Figure 5. Image restoration for EDM notches in a cast stainless steel block, from left to right : original data  $F$ , experimental data  $G$ , MAP restored image.

## CONCLUSION

In this work, we find that the Groshong model is an ideal empirical model for image processing: it is easy to code while the analytical expression for the gradient speeds up the restoration process. However, this model cannot provide any information on the defect depths and the procedure for the parameters estimation can be troublesome for noisy data. The stochastic optimization method (simulated annealing) used for parameter estimation is proved to be accurate. The time required for this should not be a serious handicap for practical purposes since it need be carried out only once for each experimental configuration. The Gauss-Markov random fields appear to be a powerful tool for representing our *a priori* knowledge of the noise and signal in a clear statistical framework. Finally, the MAP restoration method is efficient for recovering the shape of defects from noisy data and thus facilitates EC signal evaluation.

## REFERENCES

1. B.R. Groshong, G.L. Bilbro and W.E. Snyder, J. Nondestr. Eval., Vol. 10, p. 55, 1991.
2. B.R. Groshong, G.L. Bilbro and W.E. Snyder, J. Nondestr. Eval., Vol. 10, p. 127, 1991.
3. B.R. Groshong, "Eddy Current Image Restoration", Ph.D. Thesis, North Carolina State University, 1990
4. J. S. Lim, *Two-Dimensional Signal and Image Processing* (Prentice Hall, Englewoods Cliffs, 1990), Chap. 6.
5. S. Kirkpatrick, C.D. Gelatt and Jr. M. P. Vecchi, Science, Vol. 220, p. 671, 1983.
6. E. Walter and L. Pronzato, *Identification de Modèles Paramétriques à partir de Données Expérimentales* (Masson, Paris, 1994), Chap 3.
7. G. Demoment, IEEE Trans. Acoust. Speech Sig. Pro., Vol 37, No 12, p. 2024, 1989.
8. J. Besag, J. R. Statist. Soc. B, Vol. 48, No 3, p. 259, 1986.
9. S. Geman and D. Geman, IEEE Trans. Pattern Analy. Machine Intel., Vol. 6, No 6, p. 721, 1984.
10. Z. Wu and R. Leahy, IEEE Trans. Image Proces., Vol. 2, No 4, p. 520, 1993.
11. P. Loubaton, Traitement du signal, Vol. 6, N° 4, p. 223, 1989.
12. C. Bouman, IEEE Trans. Image Proces., Vol. 2, No 3, p. 296, 1993.
13. T. Sollier, R. Besnard, D. Villard, C. Chavant and D. François, 6<sup>th</sup> European Conf. NDT, Nice, France, 1994.